Article

Not peer-reviewed version

A Tomato Leaf Curl New Delhi Virus Vector for Virus-Induced Gene Silencing in Melon

Yufei Han , Rong Zeng * , Fuming Dai * , Ping Gao , Liqing Zhang , Bingqian Wan , Lihui Xu , Shigang Gao , Zhiwei Song

Posted Date: 17 September 2025

doi: 10.20944/preprints202509.1263.v1

Keywords: melon; tomato leaf curl new Delhi virus; virus-induced gene silencing; phytoene desaturase gene

 doi:10.20944/preprints202509.1263.v1

Article

A Tomato Leaf Curl New Delhi Virus Vector for Virus-Induced Gene Silencing in Melon

Yufei Han [1], Ping Gao [2], Liqing Zhang [2], Bingqian Wan [2], Lihui Xu [2], Shigang Gao [2], Zhiwei Song [2], Rong Zeng [2,*] and Fuming Dai [2,*]

[1] College of Fisheries and Life Sciences, Shanghai Ocean University, Shanghai 201306, China

[2] Eco-Environmental Protection Research Institute, Shanghai Academy of Agricultural Sciences, Shanghai 201403, China

* Correspondence: zengrong@saas.sh.cn (R.Z.); fumingdai@163.com (F.D.)

Abstract

In this study, the insert length, location within the coat protein-encoding gene, and sequence orientation of the target fragment were optimized to construct an efficient virus-induced gene silencing (VIGS) system in melon using a tomato leaf curl New Delhi virus (ToLCNDV) vector. The melon phytoene desaturase gene (*CmPDS*), a key regulator of chlorophyll biosynthesis, was selected as a reporter gene to evaluate the effects of the VIGS system. Our results revealed that the melon leaves in all the VIGS treatments exhibited a typical photobleaching phenotype at 21 days post-inoculation. Moreover, reverse transcription quantitative real-time PCR revealed a significant reduction in the mRNA levels of PDS in melon. The highest silencing efficiency (lowest PDS mRNA levels) was achieved by the VIGS vector harboring a 165 bp CmPDS fragment at the 3′ end of the AV1 gene. These findings will be highly important for the development of novel ToLCNDV-based silencing vector tools and their application to functional genomics and cucurbit crop disease resistance breeding research in the future.

Keywords: melon; tomato leaf curl new Delhi virus; virus-induced gene silencing; phytoene desaturase gene

1. Introduction

Melon (*Cucumis melo* L.) is a globally significant economic crop. The validation of gene functions in melon relies primarily on stable genetic transformation systems. However, genetic transformation efficiency in melons is significantly hindered by genotype-specific constraints, which severely restricts the application of breeding strategies. Virus-induced gene silencing (VIGS), a reverse genetics tool developed on the basis of plant antiviral mechanisms, has been widely applied in plant gene functional studies because of its independence from plant genetic transformation systems, short experimental cycles, simplicity of operation, and ability to silence single gene or gene family members [1–3]. Its principle involves the insertion of specific fragments of target genes into viral vectors, the use of viral replication and transmission capabilities to induce the silencing of endogenous genes in plants, and the inference of gene functions through resulting phenotypic or physiological changes [2–4]. Currently, VIGS vectors for cucurbit crops rely primarily on RNA viruses, such as Tobacco rattle virus (TRV) [5,6], Tobacco ringspot virus (TRSV) [7], and Cucumber green mottle mosaic virus (CGMMV) [8]. Among these, the silencing efficiency, infection range, and stability of VIGS vectors constructed using TRV are particularly outstanding, making them the most widely applied tools for gene silencing [9–11]. However, the use of RNA viruses as VIGS vectors is limited because of their inherent structural instability and susceptibility to degradation during in vitro synthesis.

Compared with RNA viral vectors such as TRV, DNA viral vectors offer distinct advantages: they do not require in vitro transcription to synthesize RNA viral chains, are more stable, and are less prone to degradation during carrier preservation than RNA vectors are. Additionally, compared with

 doi:10.20944/preprints202509.1263.v1

RNA genomes, DNA genomes are inherently more stable, have lower mutation rates, and ensure higher fidelity of foreign expressed products [12]. Currently, the majority of research efforts on engineering DNA viruses as VIGS vectors have focused on geminiviruses. Geminivirus-based vectors exhibit a rapid replication capacity for exogenous small dsRNA fragments, enabling efficient gene silencing. Notably, their modular genomic components are amenable to genetic engineering, making these viruses an ideal platform for VIGS applications. Multiple geminiviruses, including Abutilon mosaic virus (AbMV), African cassava mosaic virus (ACMV), Tomato yellow leaf curl China virus (TYLCCNV), Cotton leaf crumple virus (CLCrV), Tomato golden mosaic virus (TGMV), Bhendi yellow vein mosaic virus (BYVMV), and Cabbage leaf curl virus (CaLCV) [13–19], have been successfully employed as VIGS vectors to silence genes involved in chlorophyll synthesis in host plants, demonstrating their robust functional utility in plant molecular biology studies. However, current research has focused primarily on Nicotiana benthamiana, with melon-related studies remaining relatively limited.

Tomato leaf curl New Delhi virus, a bipartite single-stranded DNA virus belonging to the Geminiviridae family, genus Bean golden yellow mosaic virus [20–22], consists of two circular DNA components (DNA-A and DNA-B) ranging from 2,600 to 2,800 nucleotides. DNA-A encodes viral replication-related proteins, including those required for replication, gene expression regulation, and capsid formation, providing ideal insertion sites for exogenous gene fragments. The open reading frame (ORF) encoded by DNAB is associated with viral movement within and between host plant cells [23–25], enabling efficient systemic infection capacity. ToLCNDV has a broad host range and is highly infectious and can infect various crops (e.g., Solanaceae and Cucurbitaceae), ornamental plants (e.g., chrysanthemum), weeds, and wild plants [26–29]. Phytoene desaturase (PDS) is a key enzyme in the carotenoid biosynthesis pathway. It is commonly used as an indicator gene in VIGS studies because of its silencing-induced photobleaching phenotype in plant leaves caused by carotenoid deficiency [30–32]. This study was based on a full-length DNA infectious clone of ToLCNDV, in which melon plants were used as the experimental material and the phytoene desaturase gene *CmPDS* was used as an indicator. The objective of this study was to systematically evaluate the effects of the length institution site with the AV1 gene (coat protein-encoding gene), and sequence orientation of the target fragment on the silencing efficiency of the ToLCNDV-mediated VIGS system. By optimizing these parameters of the target gene, this study aimed to establish an efficient VIGS technical system tailored for melon.

2. Materials and Methods

2.1. Plant, Inoculation, and Host Bacterial Materials

Melon (Tinglin) seedlings with only two cotyledons were used for ToLCNDV-VIGS gene silencing trials.

pCambia-ToLCNDV-1.3A and pCambia-ToLCNDV-1.6B were the infectious clones of ToLCNDV DNA-A and DNA-B, respectively, and were used for ToLCNDV infection of melon by artificial inoculation [11].

Escherichia coli strain T1 and Agrobacterium tumefaciens strain GV3101 were purchased from Shanghai WEIDI Biotech Co., Ltd.

2.2. Design of Target Fragments and Construction of Vacant Vectors

The coding sequence (CDS) of the PDS gene was selected as the target gene for silencing in melon. PDS sequences from melon, cucumber, watermelon, and other members of the Cucurbitaceae family were retrieved from the NCBI GenBank database and aligned using the software MegAlign 5 [33]. The conserved PDS sequence in melon was selected for designing candidate gene sequence fragments for silencing assessment.

Special restriction enzyme recognition sites were designed by SnapGene software [34], and are absent in both the infectious clone vector pCambia-ToLCNDV-1.3A and the target fragments. Before

 doi:10.20944/preprints202509.1263.v1

the ToLCNDV-VIGS vectors were constructed, two vacant vectors (pCambia-SSNK and pCambia-NB) were constructed from pCambia-ToLCNDV-1.3A to ensure equivalence of the lengths of the reorganized AV1 gene.

2.3. Construction of ToLCNDV-Based VIGS Vectors

2.3.1. Construction of VIGS Vectors with Different Target Fragment Lengths

The vacant vector pToLCNDV-SSNK and four *CmPDS* fragments were digested with the restriction endonucleases *Nco* I and *Kpn* I. Then, the linearized vector was ligated to each digested target fragment. Four VIGS vectors were constructed, in which the middle region of the AV1 gene was substituted with 288 bp, 165 bp, 87 bp, and 48 bp CmPDS fragments.

2.3.2. Construction of VIGS Vectors with Different Substitution Areas for the CmPDS Fragment

The optimal size of the target fragment can be determined on the basis of the results from Step 2.3.1. For this purpose, the vector pToLCNDV-NB and the target fragment of optimal size were digested with *Nco* I and *BstE* II, whereas the vector pToLCNDV-SSNK and the optimal target fragment were digested with *Spe* I and *Sma* I. These modifications generated two additional vectors containing target fragments of optimal size with 3′ end substitution and 5′ end substitution, respectively. The VIGS vectors with middle region substitution were previously constructed in Section 2.3.1.

2.3.3. Construction of VIGS Vectors with the Antisense Orientation of CmPDS Fragments

On the basis of the framework from Steps 2.3.1, 165 bp, 87 bp, and 48 bp, the CmPDS fragment in the sense orientation was replaced with its antisense counterpart, and VIGS vectors carrying *CmPDS* fragments in the antisense orientation were constructed using the same method.

2.4. Agroinfiltration

The *A. tumefaciens* cultures of each VIGS vector, vacant vectors (pToLCNDV-SSNK and pToLCNDV-NB) and pCambia-ToLCNDV-1.6B, were adjusted to an optical density (OD600) of 1.0. Then, the suspensions of the VIGS vector and the vacant vector were mixed with pCambia-ToLCNDV-1.6B suspensions individually at a 1:1 volume ratio and incubated at 28°C in the dark for 3 h before infiltration into melon plants [35].

Inoculation was performed using the cotyledon injection method [8]. The experiment involved three treatments: VIGS vector inoculation (including the CmPDS fragment), a negative control (pToLCNDV-SSNK and pToLCNDV-NB) and a blank control (infiltration buffer). The treatments were set in three repetitions, each including 16 melon plants. After inoculation, the plants were grown immediately under the first 24 h in the dark and then under normal growth conditions with a 16 h light/8 h dark photoperiod [35].

2.5. Effects of VIGS Vectors on the Phenotypic Traits of Melon Plants

The number of melon plants displaying photobleaching phenotypes in each VIGS treatment was recorded at 21-day post-inoculation (dpi). The plants in the VIGS treatment group that exhibited the most obvious photobleaching phenotype were selected and grown under the same conditions for further observation of systemic silencing for three months.

2.6. Effects of VIGS Vectors on PDS Gene Expression in Melon

Apical leaves from each treatment group were selected at 9 and 21 dpi, after which total RNA was extracted and reverse-transcribed into cDNA. The relative expression level of the PDS gene in melon was determined using reverse transcription quantitative real-time PCR (RT–qPCR) with the primer set *CmPDS*-qPCR-F (5′-GCAATGCTTGGTGGGCAATC-3′) and *CmPDS*-qPCR-R (5′-

 doi:10.20944/preprints202509.1263.v1

GATTCCTGCAGCTTCCATACC-3′), while the expression of the *actin* gene (used as an internal reference) of cucurbit plants was determined by the primer set *CuActin*-qPCR-F (5′-CGGGAAATTGTCCGTGACAT-3′) and *CuActin*-qPCR-R (5′-GATTCCTGCAGCTTC CATACC-3′). Each reaction contained a negative control with nuclease-free water as the template. Relative expression levels were calculated using the $2^{-}\Delta\Delta Ct$ method, and the negative control was set to an arbitrary value (1.0) [8].

3. Results

3.1. Design of Target Fragments and Construction of Vacant Vectors

A highly conserved 288 bp-CDS from the PDS gene of melon was selected as a candidate target fragment. Four fragments of different lengths (288 bp, 165 bp, 87 bp, and 48 bp) from the 288 bp-CDS above were used as the substitution fragments. Five restriction enzymes (*Spe* I, *Sma* I, *Nco* I, *Kpn* I, and *BstE* II) were selected, and their enzyme recognition sequences were added to the 5′ and 3′ ends of the substitution fragments (Table A1).

The vector pToLCNDV-SSNK, containing *Spe* I, *Sma* I, *Nco* I, and *Kpn* I recognition sites, is designed to insert target fragments (including forward and reverse orientations) into the central and 5′ regions of the *AV1* gene (Figure 1a), whereas pToLCNDV-NB, containing *Nco* I and *BstE* II recognition sites, is specifically used to construct VIGS vectors with target fragments positioned at the 3′ ends of the *AV1* gene (Figure 1b).

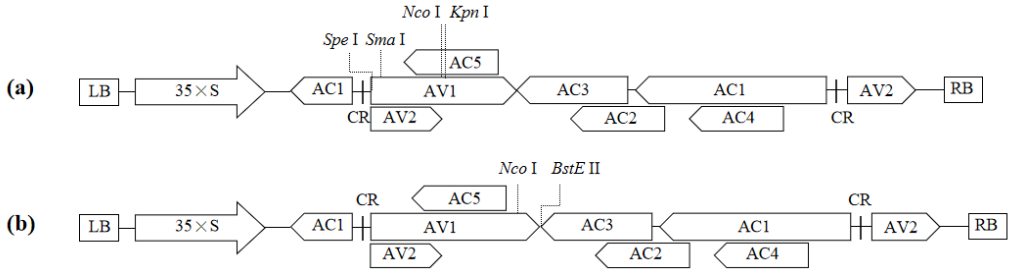

Figure 1. Schematic diagram of the two vacant vectors used for constructing the VIGS vectors. **(a)** Vector pToLCNDV-SSNK. **(b)** Vector pToLCNDV-NB.

3.2. Construction of ToLCNDV-Based VIGS Vectors

In the central region of the viral AV1 gene within pToLCNDV-SSNK, a 6 bp sequence was substituted with *CmPDS* fragments in the sense orientation (288 bp, 165 bp, 87 bp, and 48 bp) and antisense orientation (165 bp, 87 bp, and 48 bp). The VIGS vectors used were pToLCNDV-288*CmPDS*-NK, pToLCNDV-165*CmPDS*-NK, pToLCNDV-87*CmPDS*-NK, pToLCNDV-48*CmPDS*-NK, pToLCNDV-165*CmPDS*-RC-NK, pToLCNDV-87*CmPDS*-RC-NK, and pToLCNDV-48*CmPDS*-RC-NK (Figure. 2a).

In the 5′ region of the viral AV1 gene within pToLCNDV-SSNK, a 30 bp sequence was substituted with a 165 bp CmPDS fragment, resulting in the construction of the pToLCNDV-165*CmPDS*-SS vector (Figure. 2b).

In the 3′ region of the viral AV1 gene within pToLCNDV-NB, a 95 bp sequence was substituted with a 165 bp CmPDS fragment, resulting in the construction of the vector pToLCNDV-165*CmPDS*-NB (Figure. 2c).

 doi:10.20944/preprints202509.1263.v1

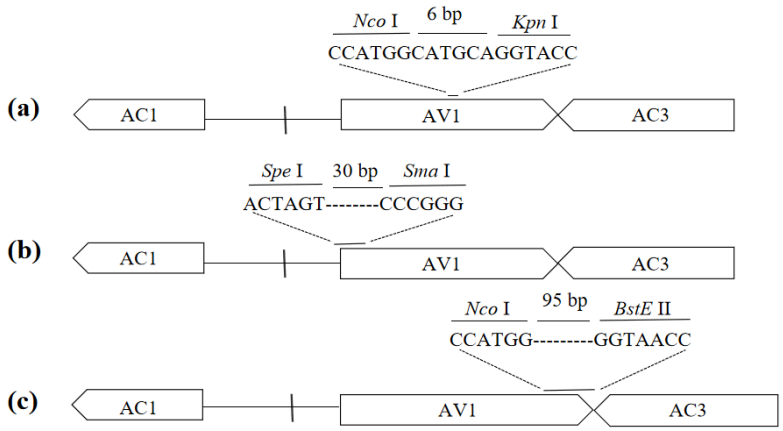

Figure 2. Engineering of VIGS vectors on three different locations of the AV1 gene substituted by the target fragment. '—' represents the target fragment. **(a)** Middle substitution. **(b)** 5′ end substitution. **(c)** 3′ end substitution.

3.3. Effects of VIGS Vectors on Melon Leaf Photobleaching

Melon plant phenotypes were photographed at 9, 21, and 90 dpi. At 9 dpi, melon plants with 165-bp- target fragment treatment (pToLCNDV-165*CmPDS*-NK, pToLCNDV-165*CmPDS*-NB, pToLCNDV-165*CmPDS*-SS and pToLCNDV-165*CmPDS*-RC-NK) exhibited a marked photobleaching phenotype, whereas those subjected to other VIGS treatments did not present the same phenotypes (Figure 3a). At 21 dpi, among the VIGS treatments with different sizes of target fragments, the vector containing the 165 bp *CmPDS* fragment resulted in the greatest number of plants whose most pronounced photobleaching symptoms were systemically silenced (Table 1; Figure 3a). Furthermore, compared with the 5′ end substitution, the pToLCNDV-165*CmPDS*-NB and pToLCNDV-165*CmPDS*-SS vectors achieved systemic silencing frequencies of 100.00% and 79.17%, respectively (Table 1), indicating that the 3′ end substitution yields a superior systemic silencing frequency. The photobleaching phenotypes in the leaf tissues were consistent with the systemic silencing results (Figure 3b). Antisense- and sense-targeted VIGS vectors resulted in comparable systemic silencing frequencies (Figure 3c). Melon plants in the check controls exhibited no significant photobleaching (Figure 3d).

To investigate the long-term gene silencing stability of the ToLCNDV-based VIGS vector during extended growth periods, we cultured pToLCNDV-165*CmPDS*-NB-treated plants for three months. The newly emerged leaves and flowers of these plants also displayed photobleaching phenotypes (Figure 3e).

Table 1. Percentage of melon plants whose expression was systemically silenced.

VIGS Sytems (with pCambia-ToLCNDV-1.6B)	Systemically silenced plants/total infiltrated plants	Systemic silencing frequency in average*
pToLCNDV-288*CmPDS*-NK	14/16, 14/16, 15/16	89.58% ± 3.61%
pToLCNDV-165*CmPDS*-NK	15/16, 15/16, 16/16	95.83% ± 3.61%
pToLCNDV-87*CmPDS*-NK	13/16, 14/16, 13/16	83.33% ± 3.61%
pToLCNDV-48*CmPDS*-NK	14/16, 13/16, 12/16,	81.25% ± 6.25%
pToLCNDV-165*CmPDS*-NB	16/16, 16/16, 16/16,	100.00% ± 0%
pToLCNDV-165*CmPDS*-SS	13/16, 12/16, 13/16	79.17% ± 3.61%
pToLCNDV-165*CmPDS*-RC-NK	14/16, 15/16, 16/16	93.75% ± 6.25%
pToLCNDV-87*CmPDS*-RC-NK	14/16, 12/16, 13/16,	81.25% ± 6.25%
pToLCNDV-48*CmPDS*-RC-NK	13/16, 13/16, 14/16	83.33% ± 3.61%

* The values following the ± denote standard deviation (SD).

 doi:10.20944/preprints202509.1263.v1

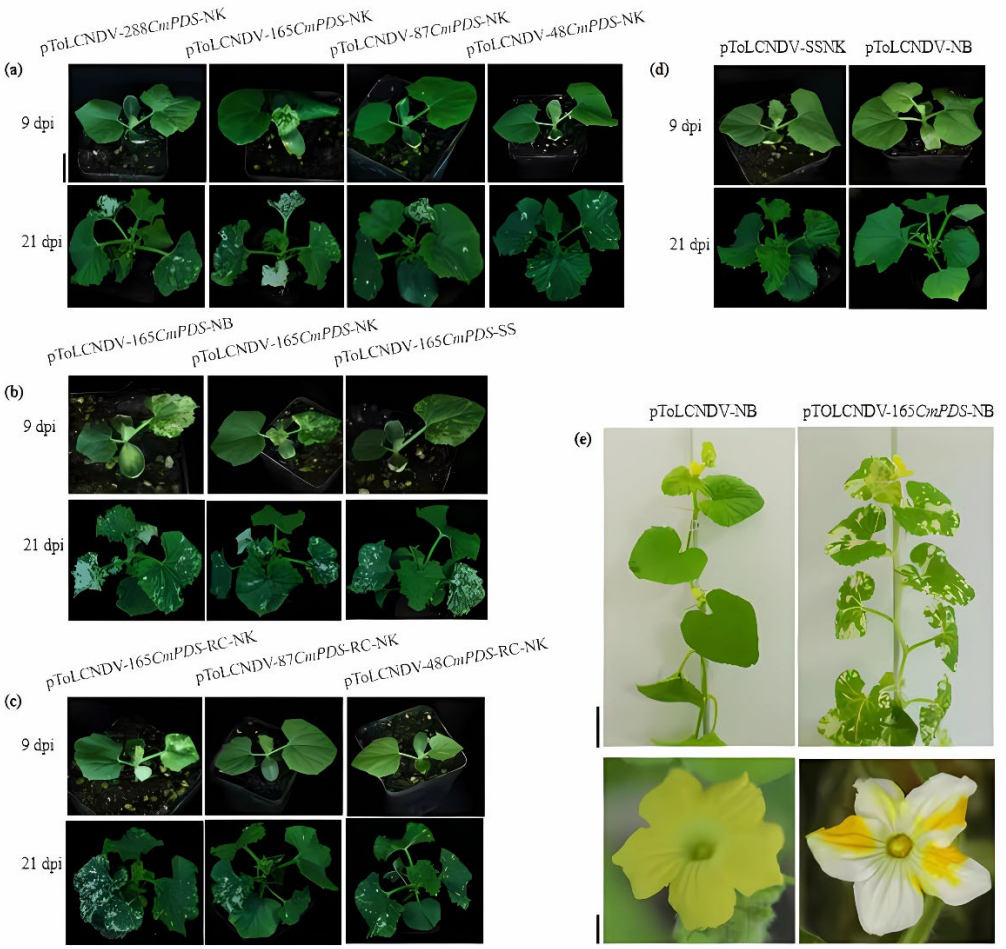

Figure 3. Phenotypic alterations in melon plants after inoculation. **(a)** Leaf photobleaching in response to VIGS treatments with varying target fragment lengths. **(b)** Leaf photobleaching in the VIGS treatments with the 165 bp *CmPDS* fragment substituting different areas of the *AV1*gene. **(c)** Leaf photobleaching in the VIGS treatments with the *CmPDS* fragment inserted in the antisense orientation of different lengths. **(d)** Leaf phenotype in the control treatments. **(e)** Systemic silencing phenotype in newly emerged leaves and flowers after pToLCNDV-165*CmPDS*-NB treatment. Bar = 2 cm, 5 cm, and 1 cm.

3.4. Influence of VIGS Vectors on PDS Gene Expression in Melon

3.4.1. Silencing Effects of the Length of the CmPDS Fragment

To investigate the impact of target fragment length on gene silencing efficiency, RT–qPCR was performed to analyze the mRNA accumulation of the *PDS* gene. The results revealed that all the VIGS treatments resulted in significantly fewer pToLCNDV-NK cells at 9 and 21 dpi ($p < 0.0001$). In addition, compared with the other VIGS treatments, the pToLCNDV-165*CmPDS*-NK treatment resulted in the most significant reduction in PDS expression at both 9 and 21 dpi (Figure 4a). Compared with the pToLCNDV-NK and pToLCNDV-48*CmPDS*-NK treatments, the pToLCNDV-288*CmPDS*-NK treatment also resulted in significantly lower *PDS* expression ($p < 0.05$), while the expression of the latter two vectors did not significantly differ. These findings suggested that the 165 bp target fragment achieved maximum silencing efficiency.

 doi:10.20944/preprints202509.1263.v1

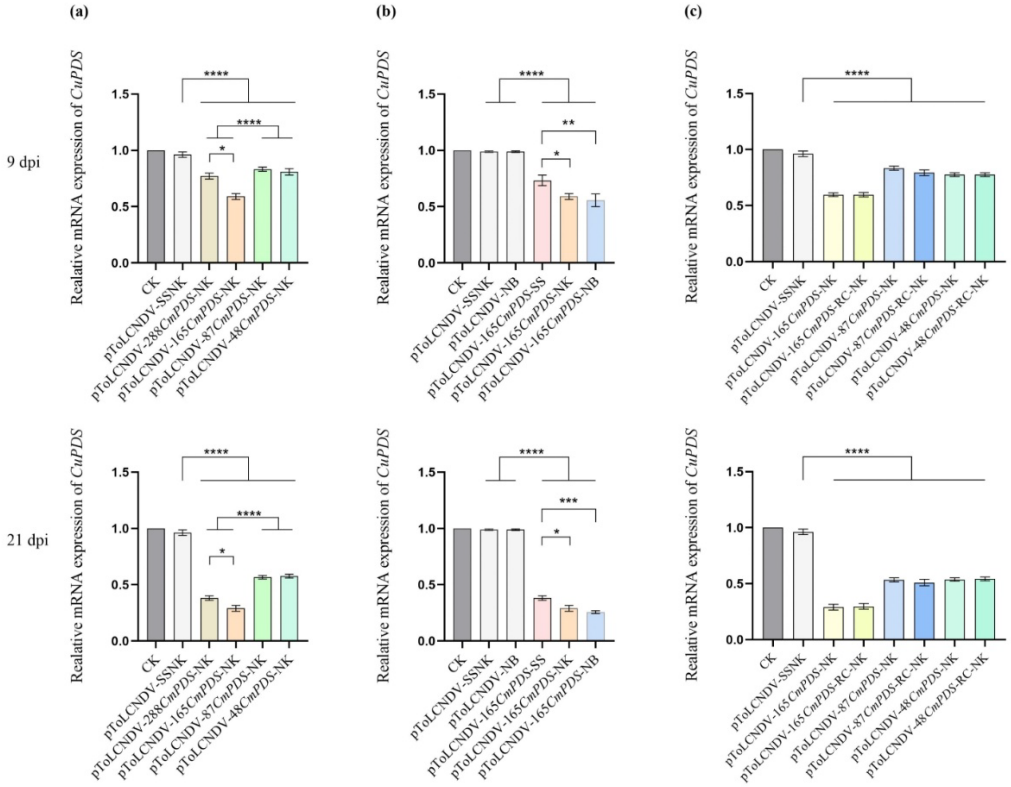

Figure 4. Real-time qRT–PCR analysis of *PDS* expression in melon plants after VIGS treatment. Three technical replicates were performed for each individual sample. Significant differences between the samples in a pair are indicated as follows: *: $P < 0.05$, **: $P < 0.001$, ***: $P < 0.001$, ****: $P < 0.0001$ by Student's t test. The error bars indicate the SDs. **(a)** Silencing efficiency of VIGS vectors carrying *CmPDS* fragments of different sizes. **(b)** Silencing efficiency of VIGS vectors with 165 bp *CmPDS* fragments substituting different areas of the *AV1* gene. **(c)** Silencing efficiency of VIGS vectors with 165 bp, 87 bp, and 48 bp *CmPDS* fragments in the sense and antisense orientation.

3.4.2. Silencing Effects of the Substitution Area of the CmPDS Fragment

To further evaluate the influence of the area of the target fragment within the *AV1* gene on VIGS efficiency, RNA samples from the pToLCNDV-165*CmPDS*-NB, pToLCNDV-165*CmPDS*-SS, and pToLCNDV-165*CmPDS*-NK treatments were analyzed. The results revealed that compared with those in the pToLCNDV-165*CmPDS*-SS treatment group, the amounts in the pToLCNDV-165*CmPDS*-NB and pToLCNDV-165*CmPDS*-NK treatment groups were significantly lower at 9 dpi ($p < 0.01$ and $p < 0.05$, respectively). Moreover, the differential expression levels of *PDS* between the pToLCNDV-165*CmPDS*-NB and pToLCNDV-165*CmPDS*-SS treatments further increased at 21 dpi ($p < 0.001$). These findings confirmed that compared with 5′ end insertion, the VIGS system with 3′ end insertion resulted in greater silencing efficiency.

3.4.3. Silencing Effects of CmPDS Fragments in the Antisense Orientation

The effects of target fragment sequence orientation on silencing efficiency were also evaluated. The results revealed that the *PDS* expression levels in the antisense-targeted VIGS vectors (pToLCNDV-165*CmPDS*-RC-NK, pToLCNDV-87*CmPDS*-RC-NK, and pToLCNDV-48*CmPDS*-RC-NK) did not significantly differ from those in the corresponding sense-targeted VIGS vectors at either 9 or 21 dpi. The results demonstrated that the sequence orientation of the target fragment did not significantly affect the gene silencing efficiency of the ToLCNDV-based VIGS system.

4. Discussion

 doi:10.20944/preprints202509.1263.v1

In this study, we successfully engineered ToLCNDV as a VIGS vector and effectively silenced the *PDS* gene in melon. We systematically investigated the impact of the insertion length, position within the AV1 gene, and sequence orientation of the target fragment on gene silencing. Our results demonstrated that the target fragment insertion length was the critical factor for the ToLCNDV-VIGS system and further revealed that the ToLCNDV-based VIGS system is capable of sustainably inducing gene silencing in melon. To the best of our knowledge, this is the first application of ToLCNDV as a VIGS vector for endogenous gene silencing in melon.

The insertion of target gene fragments of excessive length in viral vectors tends to destabilize the viral genome, impairing infectivity and increasing off-target effects. Conversely, overly short inserts compromise vector stability, resulting in efficiency reduction [36–38]. Previous research has successfully engineered ACMV and AbMV into a VIGS vector, demonstrating that the DNA-A component lacking the AV1 gene can achieve systemic spread in planta when it is co-administered with DNA-B [13,14]. We initially positioned the exogenous gene within the central region of the *AV1* gene to construct VIGS vectors harboring target fragments of varying lengths. Our results showed that VIGS vectors with 288, 165, 87, and 48 bp target fragments efficiently silenced the *PDS* gene (reducing *PDS* transcript levels by 50–75%), with 165 bp achieving the greatest silencing—slightly deviating from the reported optimal range of 200–350 bp [39–42]. For example, employing barley striped mosaic virus (BSMV) as a VIGS vector to silence the *PDS* gene revealed that the optimal insert lengths were approximately 200 bp in barley [39] and 275 bp in wheat [40]. In TRV-based VIGS studies, the insertion of a 255-bp *JrPOR* (protochlorophyllide reductase) fragment elicited the most pronounced photobleaching phenotype in walnut [41], whereas the introduction of a 301-bp cDNA fragment enabled efficient silencing of the *PDS* gene in soybean [42]. However, when TYLCCNV was engineered as a VIGS vector to silence the *GFP* and *PDS* genes in 16c tobacco, an optimal insert length of 170 bp was identified [15], which is consistent with our findings.

The position of the target fragment within the *AV1* gene also influences the viability, stability, infectivity, and silencing efficiency of the VIGS vector [8]. Next, we repositioned the exogenous gene at both the 5′ and 3′ ends of the *AV1* gene to construct VIGS vectors. Our work revealed that compared with the 5′ end substitution, the 3′ end and mid-region substitutions in this study resulted in significantly higher systemic silencing frequency and silencing efficiency. These results indicate that positioning the insertion site proximal to the 3′ end of the *AV1* gene significantly enhances viral replication and accumulation efficiency. This may be closely tied to the gene architecture and the distribution of functional elements. The 3′ non-transcribed region (UTR) often contains regulatory elements, and the insertion of target genes into this region minimizes interference with viral replication and systemic movement [43]. In contrast, insertions near the 5′ end (coding region) may disrupt the translation of critical viral proteins, such as promoters, thereby reducing viral replication capacity and silencing efficiency [44]. For example, the same 3′ UTR of the coat protein-encoding gene insertion strategy has been proven to efficiently express greater amounts of foreign genes when citrus tristeza virus (CTV) and lettuce infectious yellows virus are used [45,46]. In this study, the central region insertion within the *AV1* gene also affected the *AC5* gene, which is associated with gene silencing suppression [11], while the 5′ end insertion influenced the *AV2* gene (encoding the movement protein). This also explains the higher silencing efficiency observed in VIGS vectors constructed with central-region insertion than in those constructed with 5′ end insertion.

The sequence orientation of the target gene may impact the silencing efficiency of the VIGS vectors. Some reports have demonstrated that antisense inserts can achieve greater silencing than those with sense insertion can when the bean pod mottle virus (BPMV) system [47], brome mosaic virus (BMV) system [48], CTV system [49], and rice tungro bacilliform virus (RTBV) system are used [50], whereas other studies have suggested that silencing efficiency is not influenced by the insert orientation when the barley stripe mosaic virus (BSMV) system [51], tobacco mosaic virus (TMV) system [52], cabbage leaf curl virus (CaLCuV) system [53], or TRV-VIGS system are used [54]. To further study the impact of the insertion orientation of the ToLCNDV-VIGS system on silencing efficacy, we inserted 165-, 87-, and 48-bp antisense target fragments within the central region of the

 doi:10.20944/preprints202509.1263.v1

AV1 gene. Our results suggest that compared with sense insertions, antisense insertions resulted in equivalent silencing.

5. Conclusions

In this report, the conditions for efficient virus-mediated gene silencing in melon were optimized using the ToLCNDV-VIGS system. To achieve the most efficient gene silencing, the best combination is to insert a 165 bp target fragment into the 3′ end of the *AV1* gene within ToLCNDV. These findings will be highly meaningful when the gene functions of melon and other cucurbits crops, particularly those with limited genetic transformation tools, are applied in the future.

Author Contributions: Conceptualization, Y.H. and R.Z.; supervision, Y.H., R.Z. and F.D.; methodology, Y.H., P.G. and R.Z.; software, Y.H., S.G. and L.Z.; guidance for experimental, R.Z. and F.D.; test sample processing and collection—Y.H. and Z.S.; experimental operation—Y.H. and B.W.; writing—original draft preparation, Y.H., P.G. and F.D.; writing—review and editing, Y.H., R.Z. and F.D.; funding acquisition—R.Z. and F.D. All authors have read and agreed to the published version of the manuscript.

Funding: This work was supported by: Project of Eco-Environmental Protection Research Institute, SAAS (JB-02); Agriculture Research System of Shanghai, China (Grant No. 202501).

Data Availability Statement: The original contributions presented in this study are included in the article. Further inquiries can be directed to the corresponding author(s).

Conflicts of Interest: The authors declare no conflicts of interest.

Appendix A

Table A1. Sequence, restriction enzyme at two ends, and positions of target fragments within AV1 gene used to construct VIGS vectors.

Target fragment	Sequences(5′→3′)	Restriction Enzymes at the 5′ end	Restriction Enzymes at the 3′ end	Inserting position Within *AV1*gene
288*CmPDS*-NK	atggcgttttggggtagtgagattgtgggcgatgggttgaaag tatctggcagacatgttagtaggaaactgtataagggagctat accactgaagatagtttgtgtggattaccctagaccacagatag atgatacagttaatttcattgaagcagcttccatatctgctagtttt cgtgcttctgcacgtcccaggaagccattgaaagtagtgattgc tggggcaggattggctggtatatcgacagcaaaatatttggca gatgctggccacaaacctgttcat	*Nco* I	*Kpn* I	middle
165*CmPDS*-NK	atggcgttttggggtagtgtgttagtaggaaactgtataaggg agctataccactgaagatagtttgtgtggattaccctagaccac agatagatgatacagttaatttcattgaagcagcttccata	*Nco* I	*Kpn* I	middle
87*CmPDS*-NK	gcgttttggggtagtgagattgtgggcgatgggttgaaagtat ctggcagacatgttagtaggaaactgtataagggagctata	*Nco* I	*Kpn* I	middle
48*CmPDS*-NK	gcgttttggggtagtgagattgtgggcgatgggttgaaagtat ctggc	*Nco* I	*Kpn* I	middle
165*CmPDS*-NB	cttcgcacctgcagaagagtggatttctcggagtgactcggac attattgatgcgacaatggtggaactagctaaactatttcctgat gaaatttctgctgatcagagcaaagctaagattgtgaagtacca cgttgttaaaaccccaaggtcg	*Nco* I	*BstE* II	3′ end
165*CmPDS*-SS	atggcgttttggggtagtgagattgtgggcgatgggttgaaag tatctggcagacatgttagtaggaaactgtataagggagctat accactgaagatagtttgtgtggattaccctagaccacagatag atgatacagttaatttcattgaagcagcttccata	*Spe* I	*Sma* I	5′ end
165*CmPDS*-RC-NK	tatggaagctgcttcaatgaaattaactgtatcatctatctgtggt ctagggtaatccacacaaactatcttcagtggtatagctccctta tacagtttcctactaacatgtctgccagatactttcaacccatcgc ccacaatctcactaccccaaaacgc	*Nco* I	*Kpn* I	middle

 doi:10.20944/preprints202509.1263.v1

87*CmPDS*-RC-NK	tatagctcccttatacagtttcctactaacatgtctgccagatactt tcaacccatcgcccacaatctcactaccccaaaacgc	*Nco* I	*Kpn* I	middle
48*CmPDS*-RC-NK	gccagatactttcaacccatcgcccacaatctcactaccccaaaa cgc	*Nco* I	*Kpn* I	middle

References

1. Sun, G.Y.; Ju, Y.Q.; Zhang, C.P.; Li, L.L.; Jiang, X.Q.; Xie, X.M.; Lu, Y.Z.; Wang, K.L.; Li, W. Styrax japonicus functional genomics: an efficient virus induced gene silencing (VIGS) system. Horticultural Plant Journal 2024, 10(1), 252–258.
2. Rössner, C.; Lotz, D.; Becker, A. VIGS Goes Viral: How VIGS Transforms Our Understanding of Plant Science. Annual Review of Plant Biology 2022, 73, 703–728.
3. Zulfiqar, S.; Farooq, M.A.; Zhao, T.T.; Wang, P.P.; Tabusam, J.; Wang, Y.H.; Xuan, S.X.; Zhao, J.J.; Chen, X.P.; Shen, S.X.; Gu, A.X. Virus–induced gene silencing(VIGS): a powerful tool for crop improvement and its advancement towards epigenetics. International Journal of Molecular Sciences, 2023, 24(6), 5608–5608.
4. Lisette, M.A.; Neftalí, O. Virus–Induced Gene Silencing (VIGS) in Chili Pepper (Capsicum spp.). Methods in Molecular Biology (Clifton, N.J.) 2020, 2172, 27–38.
5. Bu, R.; Wang, R.; Wei, Q.; Hu, H.Y.; Sun, H.L.; Song, P.W.; Yu, Y.A.; Liu, Q.L.; Zheng, Z.C.; Li, T.; Li, D.X.; Wang, L.; Chen, S.J.; Wu, L.L.; Wu, J.Y.; Li, C.W. Silencing of glycerol–3–phosphate acyltransferase 6 (GPAT6) gene using a newly established virus induced gene silencing (VIGS) system in cucumber alleviates autotoxicity mimicked by cinnamic acid (CA). Plant and Soil 2019, 438(1), 329–346.
6. Liao, J.J.; Wang, C.H.; Xing, Q.J.; Li, Y.P.; Liu, X.F.; Qi, H.Y. Overexpression and VIGS system for functional gene validation in oriental melon (Cucumis melo var. makuwa Makino). Plant Cell. Tissue and Organ Culture (PCTOC) 2019, 137(2), 275–284.
7. Zhao, F.M.; Lim, S.; Igori, D.; Yoo, R.H.; Kwon, S.; Moon, J.S. Development of tobacco ringspot virus–based vectors for foreign gene expression and virus–induced gene silencing in a variety of plants. Virology 2016, 492, 166–178.
8. Liu, M.; Liang, Z.; Aranda, M.A.; Hong, N.; Liu, L.M.; Kang, B.S. A cucumber green mottle mosaic virus vector for virus–induced gene silencing in cucurbit plants. Plant Methods, 2020, 16(9): 1–13.
9. Burch–Smith, T.M.; Anderson, J.C.; Martin, G.B.; Dinesh–Kumar, S.P. Applications and advantages of virus–induced gene silencing for gene function studies in plants. The Plant Journal 2004, 39(5), 734–746.
10. Zaidi, S.S.; Mansoor, S. Viral vectors for plant genome engineering. Frontiers in Plant Science 2017, 8, 539.
11. Wang, F.; Xu, Y.; Liu, X.; Shen, W.X.; Zhu, S.P.; Zhao, X.C. Use of TRV–mediated VIGS for functional genomics research in citrus. Plant Cell. Tissue and Organ Culture (PCTOC) 2019, 139(3), 609–613.
12. Domingo, E.; Holland, J.J. RNA virus mutations and fitness for survival. Annu Rev Microbiol 1997, 51, 151–178.
13. Fofana, I.B.F.; Sangare, A.; Collier, R.; Taylor, C.; Fauquet, C.M. A geminivirus–induced gene silencing system for gene function validation in cassava. Plant Mol Biol, 2004, 56: 613–624.(ACMV)
14. Krenz, B.; Wege, C.; Jeske, H. Cell–free construction of disarmed abutilon mosaic virus–based gene silencing vectors. J Virol Methods 2010, 169, 129–137.
15. Tao, X.; Zhou X. A modified viral satellite DNA that suppresses gene expression in plants. Plant J 2004, 38, 850–860.
16. Tuttle, J.R.; Idris, A.M.; Brown, J.K.; Haigler, C.H.; Robertson, D. Geminivirus–mediated gene silencing from cotton leaf crumple virus is enhanced by low temperature in cotton. Plant Physiol 2008, 148, 41–50.
17. Peele, C.; Jordan, C.V.; Muangsan, N.; Turnage, M.; Robertson, D. Silencing of a meristematic gene using geminivirus–derived vectors. Plant J 2010, 27, 357–366.
18. Jeyabharathy, C.; Shakila, H.; Usha R. Development of a VIGS vector based on the beta–satellite DNA associated with bhendi yellow vein mosaic virus. Virus Res 2015, 195, 73–78.
19. Tang, Y.; Wang F.; Zhao J.; Xie, K.; Hong, Y.; Liu, Y. Virus–based microRNA expression for gene functional analysis in plants. Plant Physiol 2010, 153, 632–641.
20. Romero, J.; Aguado, E.; Martinez, C.; Garcia, A.; Cebrian, C.; Paris, H.S.; Jamilena, M. A novel dominant resistance gene for ToLCNDV in Cucurbita spp. Acta Horticulturae 2020, 1294, 233–238.

 doi:10.20944/preprints202509.1263.v1

21. Vo, T.T.B.; Troiano, E.; Lal, A.; Hoang, P.T.; Kil, E.J.; Lee, S.K.; Parrella, G. ToLCNDV–ES infection in tomato is enhanced by TYLCV: Evidence from field survey and agroinoculation. Frontiers in Microbiology 2022, 13, 954460–954460.
22. Renukadevi, P.; Devi, G.R.; Jothika, C.; Karthikeyan, G.; Malathi, V.G., Balakrishnan, N.; Rajagopal, B.; Nakkeeran, S.; Abd–Allah, E.F. Genomic distinctiveness and recombination in tomato leaf curl New Delhi virus (ToLCNDV–BG) isolates infecting bitter gourd.3 Biotech 2024, 14(8), 184–184.
23. Martinez, C.; Manzano, S.; Megias, Z.; Garcia, A.; Garrido, R.; Paris, H.S.; Jamilena, M. Screening of Cucurbita germplasm for ToLCNDV resistance under natural greenhouse conditions.Acta Horticulturae 2017, 1151, 57–62.
24. Naveena, E.; Rajasree, V.; Behara, T.K.; Karthikeyan, G.; Kavitha, M.; Rameshkumar, D. Molecular confirmation of ToLCNDV resistance in cucumber through agroinoculation and field screening. Journal of Animal and Plant Sciences–Japs 2024, 34(6), 1582–1593.
25. Arif, M. Cross–species substitution matrix comparison of Tomato leaf curl New Delhi virus (ToLCNDV) with medicinal plant isolates. Journal of Plant Diseases and Protection 2024, 131(6), 1925–1934.
26. Iqbal, Z.; Khurshid, M. Immunocapture PCR Detection of ToLCNDV from Plant Extract by using Heterologous Virus Coat Protein Antisera. Pakistan Journal of Zoology 2017, 49(3), 1025–1031
27. Belén, R.; Pedro, G.; Dirk, J.; Ruiz, L. Insights into the Key Genes in Cucumis melo and Cucurbita moschata ToLCNDV Resistance. Horticulturae 2023, 9(2), 231–231.
28. Prasad, A.; Prasad M. Interaction of ToLCNDV TrAP with SlATG8f marks it susceptible to degradation by autophagy. Cellular and Molecular Life Sciences 2022, 79(5), 241–241.
29. Pérez–Moro, C.; Sáez C.; Sifres A.; Lopez, C.; Dhillon, N.P.S.; Picó, B.; Pérez–de–Castro, A. Genetic Dissection of ToLCNDV Resistance in Resistant Sources of Cucumis melo. International Journal of Molecular Sciences 2024, 25(16), 8880–8880.
30. Ruiz, M.T.; Voinnet, O.; Baulcomb, D.C. Initiation and maintenance of virus–induced gene silencing. The Plant Cell 1998, 10(6), 937–946.
31. Lacomme, C.; Hrubikova, K.; Ingo H. Enhancement of virus–induced gene silencing through viral–based production of inverted–repeats. The Plant journal for cell and molecular biology 2003, 34(4), 543–553.
32. Bennypaul, H.S.; Mutti, J.S.; Rustgi, S.; Kumar, N.; Okubara, P.A.; Gill, K.S. Virusinduced gene silencing (VIGS) of genes expressed in root, leaf, and meiotic tissues of wheat. Funct Integr Genomics 2012, 12, 143–156.
33. Pahlavan, A.; Solouki, M.; Fakheri, B.; Nasab, B.F. Using Morphological and Phytochemical Traits and ITS (1, 4) and rbcl DNA Barcodes in the Assessment of Different Malva sylvestris L. Genotypes. Journal of Medicinal Plants and By-Products-Jmpb, 2021, 10(1), 19–55. DOI10.22092/JMPB.2020.343520.1232.
34. Haseeb, M.; Amir, A.; Ikram, A. In Silico Analysis of SARS-CoV-2 Spike Proteins of Different Field Variants. Vaccines, 2023, 11 (4), 736. DOI10.3390/vaccines11040736.
35. Naing, H.A.; Song, Y.H.; Lee, M.J.; Lim, K.B.; Kim, C.K. Development of an efficient virus–induced gene silencing method in petunia using the pepper phytoene desaturase (PDS) gene. Plant Cell. Tissue and Organ Culture (PCTOC) 2019, 138(3), 507–515.
36. Avesani, L.; Marconi, G.; Morandini, F.; Albertini, E.; Bruschetta, M.; Bortesi, L.; Pezzotti, M.; Porceddu, A. Stability of potato virus X expression vectors is related to insert size: implications for replication models and risk assessment. Transgenic Research 2007, 16(5), 587–597.
37. Gleba, Y.; Klimyuk, V.; Marillonnet, S. Viral vectors for the expression of proteins in plants. Current Opinion in Biotechnology 2007, 18(2), 134–141.
38. Peyret, H.; Lomonossoff, G.P. When plant virology met Agrobacterium: the rise of the deconstructed clones. Plant Biotechnology Journal 2015, 13(8), 1121–1135.
39. Bruun–Rasmussen, M.; Madsen, C.T.; Jessing, S.; Albrechtsen, M. Stability of barley stripe mosaic virus–induced gene silencing in barley. Mol. Plant Microbe Interact 2007, 20(11), 1323–1331.
40. Cakir, C.; Mahmut Tör. Factors influencing barley stripe mosaic virus–mediated gene silencing in wheat. Physiol. Mol. Plant Pathol 2010, 74(3–4), 246–253.

 doi:10.20944/preprints202509.1263.v1

41. Liu, Y.; Xu, Y.; Xu, H.; Amilijiang, W.; Wang, H. Developing and applying a virus–induced gene silencing system for functional genomics in walnut (Juglans regia L.) mediated by tobacco rattle virus. Gene 2025, e936149087.
42. Deng, K.; Lu, Z.; Yang, H.;Chen, S.; Li, C.; Cao, D.; Wang, H.; Hao,Q.; Chen, H.; Shan, Z. Efficient Virus–Induced Gene Silencing (VIGS) Method for Discovery of Resistance Genes in Soybean. Plants 2025, 14, 1547–1563.
43. Liu, Y.Z.; Zhang, Y.; Wang, M.S.; Cheng, A.C.; Yang, Q.; Wu, Y.; Jia, R.Y.; Liu, M.F.; Zhu, D.K.; Chen, S.; Zhang, S.Q.; Zhao, X.X. Structures and Functions of the 3′ Untranslated Regions of Positive–Sense Single–Stranded RNA Viruses Infecting Humans and Animals. Frontiers in Cellular and Infection Microbiology 2020, 10, 453.
44. Peng, T.Y.; Yang, F.Y.; Yang, F.; Cao, W.J.; Zheng, H.X.; Zhu, Z.X. Structural diversity and biological role of the 5′ untranslated regions of picornavirus. RNA Biology 2023, 20(1), 548–562.
45. El–Mohtar C, Dawson W O. 2014. Exploring the limits of vector construction based on citrus tristeza virus. Virology, 448: 274–283.
46. Qiao, W.; Falk, B. Efficient protein expression and virus–induced gene silencing in plants using a crinivirus–derived vector. Viruses 2018, 10(5), 216.
47. Zhang, C.; Bradshaw, J.D.; Whitham, S.; Hill, J.H. The development of an efficient multipurpose bean pod mottle virus viral vector set for foreign gene expression and RNA silencing. Plant Physiol 2010, 153, 52–65.
48. Pacak, A.; Strozycki, P.M.; Barciszewska–Pacak, M.; Alejska, M.; Lacomme, C.; Jarmolowski, A.; Szweykowska-Kulinska, Z.; Figlerowicz, M. The brome mosaic virus–based recombination vector triggers a limited gene silencing response depending on the orientation of the inserted sequence. Arch Virol 2010, 155, 169–179.
49. Killiny, N.; Nehela, Y.; Hijaz, F.; Ben–Mahmoud, S.K.; Hajeri, S.; Gowda, S. Citrus tristeza virus–based induced gene silencing of phytoene desaturase is more efficient when antisense orientation is used. Plant Biotechnology Reports 2019, 13(2), 179–192.
50. Kant, R.; Dasgupta, I. Phenotyping of VIGS–mediated gene silencing in rice using a vector derived from a DNA virus. Plant Cell Reports 2017, 36(7), 1159–1170.
51. Bruun–Rasmussen, M.; Madsen, C.T.; Jessing, S.; Albrechtsen, M. Stability of barley stripe mosaic virus–induced gene silencing in barley. Mol. Plant Microbe. Interact 2007, 20, 1323–1331.
52. Hiriart, J.B.; Lehto, K.; Tyystjärvi, E.; Junttila,T.; Aro, E.M. Suppression of a key gene involved in chlorophyll biosynthesis by means of virus–inducing gene silencing. Plant Mol. Biol. 2002, 50, 213–224.
53. Xiao, Z.; Xing, M.; Liu, X.; Fang, Z.; Yang, L; Zhang, Y.; Wang, Y.; Zhuang, M.; Lv, H. An efficient virus–induced gene silencing (VIGS) system for functional genomics in Brassicas using a cabbage leaf curl virus (CaLCuV)–based vector. Planta 2020, 252, 1–12.
54. Mo, Z.H.; Chen, Y.; Zhai, M.; Zhu, K.K.; Xuan, J.P.; Hu, L.J. Development and application of a virus–induced gene silencing system for functional genomics in pecan (Carya illinoinensis). Scientia Horticulturae 2023, 310, e111759.